

Homochiral β -CF₃, -SCF₃ and -OCF₃ secondary alcohols: catalytic stereoconvergent synthesis, bioactivity and flexible crystals

Andrej Emanuel Cotman,^{*,†} Pavel A. Dub,[‡] Maša Sterle,[†] Matic Lozinšek,[§] Jaka Dernovšek,[†] Živa Zajec,[†] Tihomir Tomašič,[†] Dominique Cahard[◇]

[†] Faculty of Pharmacy, University of Ljubljana, Aškerčeva cesta 7, SI-1000 Ljubljana, Slovenia

[‡] Chemistry Division, Los Alamos National Laboratory, Los Alamos, New Mexico 87545, United States

[§] Jožef Stefan Institute, Jamova cesta 39, SI-1000, Ljubljana, Slovenia.

[◇] CNRS UMR 6014 COBRA, Normandie Université, 76821 Mont Saint Aignan, France

ABSTRACT: An optimized catalytic protocol for enantio- and diastereoselective reduction of racemic α -CF₃, α -SCF₃ and α -OCF₃ aryl ketones is described. The reaction involves a dynamic kinetic resolution (DKR) based on ruthenium catalyzed Noyori-Ikariya asymmetric transfer hydrogenation for simultaneous construction of two contiguous stereogenic centers. A range of previously inaccessible fluorinated secondary alcohols was prepared in excellent stereomeric purity (up to above 99.9% ee, up to above 99.9:0.1 dr) and in high isolated yield (up to 99%). The origin of DKR (exceptional stereoselectivity and racemization mechanism) is rationalized by density functional theory calculations. Pharmaceutically relevant further transformations of the products are demonstrated including incorporation into heat shock protein 90 inhibitor with in vitro anti-cancer activity. Moreover, needle-shaped crystals of representative stereopure products are mechanically responsive: either elastically or plastically flexible, opening the door to novel class of functional materials based on chiral molecular crystals.

Fluorine atom profoundly influences properties of bioactive molecules on multiple levels, which reflects in half of blockbuster drugs and one third of newly Food and Drug Administration-approved drugs being fluoro-pharmaceuticals.¹ Organofluorine chemistry is essentially man-made as only a dozen fluorinated natural products has been identified on Earth.² The consideration of new fluorinated chemotypes in drug development therefore inevitably follows the availability of the synthetic methods to access the relevant moieties. Outstanding progress was achieved in the preparation of a plethora of synthetic fluorine compounds.³ A less developed area being highly challenging while very rewarding is the asymmetric synthesis of stereogenic fluorinated molecules.⁴ In this context, we embarked on the asymmetric construction of chiral carbon atoms featuring a fluorinated motif with emphasis on the trifluoromethyl group C*-CF₃ and its heteroatomic homologues C*-SCF₃ and C*-OCF₃.

In particular, β -CF₃-substituted alcohols and amines are emerging motifs in medicinal chemistry (Figure 1). For example, **Compound I** as a mixture of stereoisomers exhibits antibacterial activity,⁵ and racemic **Compound II** is an inhibitor of WD repeat-containing protein 5, which is over-expressed in some types of cancer.⁶ Stereochemically defined trifluoromethylated omargliptin exhibits better pharmacokinetic and pharmacodynamic profiles compared to the parent drug molecule, and is clinically evaluated as a super long-acting antidiabetic.⁷

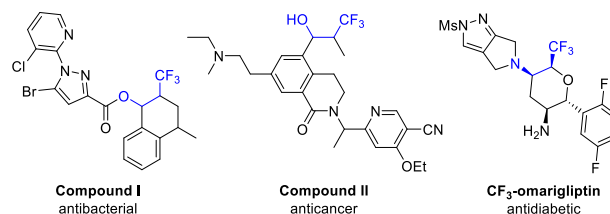


Figure 1. Bioactive compounds with β -CF₃ alcohol or amine motifs.

Given the potential of stereogenic β -CF₃-substituted alcohols and amines for medicinal chemistry applications, and eager to use them in our hit-to-lead endeavors, we were surprised to find no preceding literature reports on asymmetric synthesis of the model 2-CF₃-1-indanol **2a**, its amino analog nor their higher homologues. Non-asymmetric approaches towards such cyclic benzo-fused β -trifluoromethyl alcohols or amines received significant attention in the past five years, and are based on photoredox, electrochemical or transition metal-catalyzed oxy-trifluoromethylation⁸ or amino-trifluoromethylation⁹ of the corresponding olefins. There is only a handful of literature reports on stereoselective synthesis of β -trifluoromethyl secondary alcohol motif, based on diastereoselective hydrogenation of 2-CF₃ allylic alcohols¹⁰ or NaBH₄ reduction of stereopure α -CF₃ ketone,¹¹ or diastereoselective aldol or Reformatsky reactions using a chiral auxiliary,¹² but to the best of our knowledge no catalytic enantioselective access to this class of molecules has ever been reported.

Dynamic kinetic resolution based on Noyori-Ikariya transfer hydrogenation (DKR-ATH) seemed like a fitting synthetic strategy for addressing the challenging simultaneous control of both chiral centers of the target compound class.¹³ DKR-ATH is a robust method for stereoconvergent access to enantiomerically pure secondary alcohols with multiple contiguous chiral centers starting from the readily available racemic ketones,¹⁴ including fluorinated examples.¹⁵ Considering broad availability of the Noyori-Ikariya type ruthenium complexes (Table 1), and their relative stability towards air and moisture, this would offer not only conceptually new but also highly practical access to stereopure β -CF₃-substituted alcohols and their analogs.

Table 1. Catalyst and solvent screening for Ru(II)-catalyzed DKR-ATH of **1a**.^a

	Ru(II) cat.	F/A	Cosolvent	Time	1a:2a:3a:4a
1	(<i>R,R</i>)-C1	3:2	PhCl	3 h	0:73:19:8
2	(<i>S,S</i>)-C2	3:2	PhCl	3 h	0:75:6:19
3	(<i>S,S</i>)-C3	3:2	PhCl	3 h	0:75:19:6
4	(<i>S,S</i>)-C4	3:2	PhCl	3 h	4:55:35:6
5	(3 <i>R</i> ,1' <i>S</i>)-C5	3:2	PhCl	3 h	0:75:0:25
6	(<i>S,S</i>)-C2	3:2	-	3 h 18 h	5:24:71:0 0:25:60:16
7	(<i>S,S</i>)-C2	5:2	-	3 h 18 h	21:74:5:0 5:75:20:0
8	(<i>S,S</i>)-C2	5:2	PhCl	3 h	0:99:0:1
9	(<i>S,S</i>)-C2	5:2	DMF	3 h	0:97:0:3
10	(<i>S,S</i>)-C2	5:2	dioxane	3 h	0:98:0:2
11	(<i>S,S</i>)-C2	5:2	1,2-DCE	3 h	0:98:0:2

^aDKR-ATH of **1a** (50 mg, 0.25 mmol) was carried out using Ru(II) cat. (1 mol%), HCO₂H/Et₃N (0.25 mL) and cosolvent (0.5 mL) at 40 °C. The product ratio was determined by NMR analysis of reaction mixture aliquots, and the ratio of **2a** stereoisomers (*cis/trans* >99:1; >99% ee in all cases) was determined after isolation by ¹⁹F NMR and HPLC analysis using chiral stationary phase. F/A equals HCO₂H/Et₃N.

A model racemic ketone 2-CF₃-1-indanone **1a** was prepared in one step by triflic acid mediated annulation of benzene with 2-CF₃-acrylic acid.¹⁶ It was subjected to DKR-ATH using commonly used formic acid/triethylamine 3:2 mixture as a source of hydrogen and chlorobenzene as a co-solvent, and five representative Noyori-Ikariya type Ru(II) catalysts were tested (Table 1, runs 1–5). **C1** is the archetypical Noyori catalyst,¹⁷ and the rest are the so-called tethered catalysts, which proved to be superior for the reduction of structurally complex ketones.¹⁸ Chronologically, **C2** was developed by Wills et al.,¹⁹ followed by oxy-tethered catalyst

C3 by Ikariya et al.,²⁰ sulfamoyl-DPEN-cored **C4**,²¹ and benzosultam-cored **C5** by Mohar et al.²² The reactions using 1 mol% of catalysts **C1**–**C5** all reached >95% conversion within 3 h (Table 1, entries 1–5). Delightfully, all the catalysts yielded the product **2a** with excellent stereoselectivity²³ (*cis/trans* > 99:1 and >99% ee) as determined by ¹⁹F NMR and chiral HPLC, respectively. The absolute configuration of **2a** being (*S,S*) was determined by single-crystal X-ray diffraction (SCXRD) analysis of a product from run with (*S,S*)-**C2**. Disappointingly, significant amount of by-product, indanone **3a** and/or indanol **4a** (up to 41% total), was also detected in the reaction mixtures, indicating that an unexpected detrifluoromethylation took place during DKR-ATH. The catalysts performed differently regarding side product formation and **C2** was chosen for further studies because of its wide availability and favorable reaction kinetics (Table S1). Control experiments indicated that trifluoromethyl moiety is eliminated from the ketone **1a** rather than the product *cis*-**2a**, that it is not a ruthenium-catalyzed process, and involves formation of Et₃N/HF adduct (see SI). To mitigate fluoride elimination, the use of HCO₂H/Et₃N in 5:2 molar ratio with the most efficient (*S,S*)-**C2** was attempted. Performing the DKR-ATH in neat HCO₂H/Et₃N 3:2 or 5:2 (Table 1, entries 6 and 7) indeed revealed that by increasing the relative amount of formic acid, detrifluoromethylation level dramatically decreases while excellent stereoselectivities are still obtained. Further solvent screening revealed that the use of any cosolvent together with HCO₂H/Et₃N 5:2 was beneficial for the reaction yield as less than 3% of the side products were observed in chlorobenzene, DMF, 1,4-dioxane or 1,2-dichloroethane (Table 1, entries 8–11). The first one was deemed optimal with only 1 mol% of 1-indanol accompanying the target product **2a**.

Computational modeling was further performed to collaborate high level of stereoselectivities and realize the possible mechanism of **1a**-racemization being the core process of DKR. The reaction between **1a** and the active form of precatalyst (*S,S*)-**C2** was studied by M06-2X-D3/SMD(chlorobenzene)/def2-qzvp//def2-svp method. Four diastereomeric transition states are possible (Figure 2). For the *R*_{Ru}, λ -catalyst structural arrangement,²⁴ observed in the solid-state of (*S,S*)-**C2**,¹⁹ computations predict the ratio of the reaction rates leading to each stereoisomer as ~ 10⁹ (*S,S*) : 1800 (*R,R*) : 400 (*S,R*) : 1 (*R,S*).²⁵ This transforms into the *cis/trans* ratio of 2.5 × 10⁶ and the enantioselectivity of 99.9996% for the *cis* product.²⁶ The discrepancy between experimentally and theoretically predicted % ee is likely due to the additional mechanisms of the generation of chirality.^{27a} However, the calculation reproduces and points to high-level of stereodiscrimination. Two spatial regions of the catalyst simultaneously control the final stereoselectivity: the region of the tethered η^6 -arene ligand and the region of the SO₂ moiety.²⁷ Dynamic equilibrium and interplay of attraction and repulsion in each region through various noncovalent interactions lead to stabilization/destabilization of the corresponding stereoselectivity determining transition state. The presence of α -CF₃ functionality is crucial for exceptionally high stereoselectivity. As a comparison, DKR-ATH of 2-methyl-1-indanone using **C3** yielded the corresponding alcohol with a lower *cis*-selectivity (*cis/trans* = 98:2, 98% ee),^{14d} whereas DKR-ATH of 2-acetamido-1-indanone (hydrogen bond donor α -substituent) using **C5** was even *trans*-selective (*cis/trans* = 9:91).^{22c}

oxidative trifluoromethylation of 2-hydroxy-1-indanone.³⁶ Pushing it further, the linear analog **1q** was successfully reduced within 7 h using the same standard conditions delivering the product **2q** as a 3:1 mixture of *anti* and *syn* diastereomer with 97.4% and 90.4% ee, respectively. The reduction of 1-SCF₃-2-indanone **1r** to the corresponding alcohol **2r** was unfortunately not highly enantioselective (45% ee) although a 95:5 *cis/trans* ratio was achieved.

From medicinal chemistry point of view, the stereopure products **2** represent hitherto synthetically inaccessible building blocks featuring intrinsic non-planarity, potential for specific interactions with the protein binding sites, and several growth vectors.³⁷ Selected stereopure products **2** were thus prepared on 1 mmol scale, and relevant further synthetic transformations were demonstrated (Scheme 1). **2g** was transformed to *trans*-configured **5** via iron-catalyzed diastereoselective Friedel-Crafts benzoylation of 2-chloroanisole.³⁸ This hydroxy-substituted 1-arylindan motif is characteristic of resveratrol dimer natural products.³⁹ **2o** was converted to azide **6** (*trans/cis* = 92:8) via nucleophilic substitution (S_N2) of the corresponding mesylate ester. It was further reduced to the amine **7** which was isolated as a single stereomer after chromatography. **2i** was *O*-alkylated to get stereopure clickable building block **8**. **2d** was converted to biaryl **9** via Suzuki coupling reaction, illustrating that unprotected 2-CF₃-carbinols are compatible with palladium catalysis. And finally, stereopure **2a** and **2c** were re-oxidized using pyridinium chlorochromate to get enantioenriched **1a** and **1c** with 57% and 92% ee, respectively. To showcase direct applicability of the developed synthetic methods in a medicinal chemistry setting, alkyne **8** was incorporated in **10** that represents a novel structural class of heat shock protein 90 (Hsp90) inhibitors. Compound **10** was designed using molecular dynamics-derived pharmacophore model (Figure S2).⁴⁰ It was shown to inhibit Hsp90 in luciferase refolding assay and display antiproliferative activity in SkBr3 breast cancer cell line (IC₅₀ = 51 ± 2 μM).

Moreover, we were pleased to find out that some of the novel enantiopure compounds prepared by our method crystallize as needle-shaped crystals which are elastically (**2a**, **2d**, **2p**, **4d**) or plastically flexible (**2o**) (Figure 3, and SI). Mechanically responsive molecular crystals are being recognized as an unexplored platform for applications ranging from adaptive systems and actuators to biocompatible devices and all-organic soft robots.⁴¹ The crystal structures of **2a**, **2d**, **2o**, **2p** and **4d** exhibit some of the same features that were identified in other crystals with elastic⁴² or plastic deformation behavior.⁴³ In particular, a short crystal axis (~5 Å), anisotropic packing, corrugated crystal packing, and a prominent intermolecular interaction being highly directional (i.e., hydrogen-bonded chains parallel to the short *a*-crystallographic axis in structures with *P*2₁2₁2₁ symmetry and parallel to the short *b*-crystallographic axis in compounds crystallizing in *P*2₁ space group) with much weaker interactions in perpendicular directions. The slippage of molecular layers lined with trifluoromethyl groups has been established to be the mechanism of the observed plastic deformation.^{43c} In our case, chiral OH and indan scaffold clearly also contribute to mechanistic responsiveness as detri-fluoromethylated bromoindanol **4d** was also to some degree elastically flexible.⁴⁴ For plastically flexible **2o**, two polymorphs (RT *P*2₁, and 100 K *P*2₁2₁2₁) were identified.

Scheme 1. Further synthetic transformations of stereopure DKR-ATH products **2**.

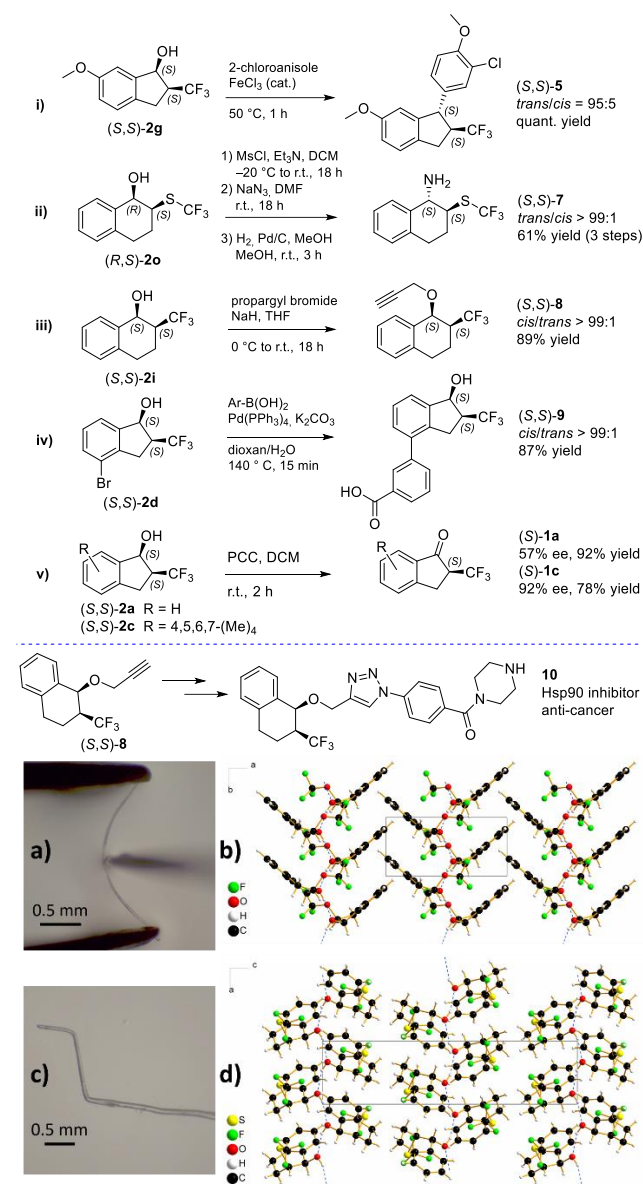


Figure 3. a) Three-point bending experiment with elastically flexible needle-shaped crystal of **2p**. b) Crystal packing of **2p**, view along *c* axis. c) Bent plastically flexible crystal of **2o**. d) Crystal packing of **2o**, view along *b* axis.

In conclusion, we have successfully developed a highly efficient dynamic kinetic resolution strategy for the Noyori-Ikariya asymmetric transfer hydrogenation of racemic α-CF₃, α-SCF₃ and α-OCF₃ aryl ketones with excellent stereoselectivities (up to above 99.9% ee, up to above 99.9:0.1 dr). The origin of DKR (in situ epimerization of the ketone substrate, and stereoselectivity) were investigated by DFT calculations. Applicability in the field of medicinal chemistry was demonstrated by several further transformations of the stereopure products including incorporation into in vitro anti-cancer compound. A new class of homochiral small organic molecules, which crystallize as mechanically responsive single-component crystals, was identified. The presented synthetic methodology opens the door to new chiral fluorinated bioactive compounds, and to material science applications based on adaptive chiral molecular crystals.

ASSOCIATED CONTENT

Supporting Information.

The supporting information is available free of charge via the Internet at <http://pubs.acs.org>.

Experimental procedures, chiral HPLC and GC chromatograms, NMR spectra of the prepared compounds, cell-based assays, computational and SCXRD details, photos of mechanically responsive behavior (PDF).

Movie 2d (AVI)

Movie 4d (AVI)

Accession codes.

CCDC 2151748–2151755 contain the supplementary crystallographic data for this paper. The data can be obtained free of charge from The Cambridge Crystallographic Data Centre via www.ccdc.cam.ac.uk/structures.

AUTHOR INFORMATION

Corresponding Author

* **Andrej Emanuel Cotman** – Faculty of Pharmacy, University of Ljubljana, Aškerčeva cesta 7, SI-1000 Ljubljana, Slovenia; Email: andrej.emanuel.cotman@ffa.uni-lj.si

Author Contributions

A. E. C., D. C., P. A. D., T. T. and M. L. conceived and planned the experiments. D. C. carried out the synthesis of fluorinated ketones, A. E. C. and M. S. carried out asymmetric reductions and product characterization, P. A. D. carried out computational mechanistic studies, T. T. and J. D. designed Hsp90 inhibitor, J. D. carried out transformations in Scheme 1, Ž. Z. performed cell-based assays, M. L. performed and interpreted SCXRD analysis and discovered flexibility of the crystals. A. E. C. took the lead in writing the manuscript with input from all authors. All authors have given approval to the final version of the manuscript.

Notes

The authors declare no competing financial interest.

ACKNOWLEDGMENT

This work was supported by the Slovenian Research Agency ARRS, Grant No. P1-0208, Z1-2635, J1-1717, Centre National de la Recherche Scientifique CNRS, Normandy University, French-Slovenian bilateral grant BI-FR/22-23-PROTEUS-004, and Los Alamos Laboratory Directed Research and Development. M. S. acknowledges Anamarija Zega as her PhD supervisor. M. L. gratefully acknowledges the funding by the European Research Council (950625). T.T. acknowledges OpenEye Scientific Software, Santa Fe, NM., for free academic licenses for the use of their software. Maja Frelih is acknowledged for acquisition of HRMS spectra.

REFERENCES

(1) a) Inoue, M.; Sumii, Y.; Shibata, N. Contribution of Organofluorine Compounds to Pharmaceuticals. *ACS Omega* **2020**, *5*, 10633–10640. b) Wang, J.; Sánchez-Roselló, M.; Aceña, J. L.; del Pozo, C.; Sorochinsky, A. E.; Fustero, S.; Soloshonok, V. A.; Liu, H. Fluorine in Pharmaceutical Industry: Fluorine-Containing Drugs Introduced to the Market in the Last Decade (2001–2011). *Chem. Rev.* **2014**, *114*, 2432–2506. c) Gillis, E. P.; Eastman, K. J.; Hill, M. D.; Donnelly, D. J.; Meanwell, N. A. Applications of Fluorine in Medicinal Chemistry. *J. Med. Chem.* **2015**, *58*, 8315–8359. d) Han, J.; Remete, A. M.; Dobson, L. S.; Kiss, L.; Izawa, K.; Moriwaki, H.; Soloshonok, V. A.; O'Hagan, D. Next Generation Organofluorine Containing Blockbuster Drugs. *J. Fluorine Chem.* **2020**, *239*, 109639. e) Mei, H.; Remete, A. M.; Zou, Y.; Moriwaki, H.; Fustero, S.; Kiss, L.; Soloshonok, V. A.; Han, J.

Fluorine-Containing Drugs Approved by the FDA in 2019. *Chin. Chem. Lett.* **2020**, *31*, 2401–2413. f) Mei, H.; Han, J.; Fustero, S.; Medd-Simon, M.; Sedgwick, D. M.; Santi, C.; Ruzziconi, R.; Soloshonok, V. A., Fluorine-Containing Drugs Approved by the FDA in 2018. *Chem. Eur. J.* **2019**, *25*, 11797–11819.

(2) Walker, M. C.; Chang, M. C. Y. Natural and Engineered Biosynthesis of Fluorinated Natural Products. *Chem. Soc. Rev.* **2014**, *43*, 6527–6536.

(3) Emerging Fluorinated Motifs: Synthesis, Properties, and Applications. Cahard, D.; Ma, J.-A. (Eds), Wiley-VCH Verlag GmbH & Co. (2020)

(4) a) Meyer, S.; Häfliger, J.; Gilmour, R. Expanding Organofluorine Chemical Space: The Design of Chiral Fluorinated Isosteres Enabled by I(I)/I(III) Catalysis. *Chem. Sci.* **2021**, *12*, 10686–10695. b) Zhu, Y.; Han, J.; Wang, J.; Shibata, N.; Sodeoka, M.; Soloshonok, V. A.; Coelho, J. A. S.; Toste, F. D. Modern Approaches for Asymmetric Construction of Carbon–Fluorine Quaternary Stereogenic Centers: Synthetic Challenges and Pharmaceutical Needs. *Chem. Rev.* **2018**, *118*, 3887–3964. c) Cahard, D.; Bizet, V., The influence of fluorine in asymmetric catalysis. *Chem. Soc. Rev.* **2014**, *43*, 135–147.

(5) Xie, R.; Wu, L. Preparation Method of Trifluoromethyl Tetralone Compound. CN111333613A, June 26, 2020.

(6) Fang, L.; Gao, Z.; Jiang, X.; Liu, K. K. C.; Mak, S. Y. F.; Oyang, C.; Wang, C.; Wang, T.; Wu, J.; Yingming, W.; Xiao, Q. Heterocyclic Wdr5 Inhibitors as Anti-Cancer Compounds. WO2021028806A1, February 18, 2021.

(7) Zhang, C.; Ye, F.; Wang, J.; He, P.; Lei, M.; Huang, L.; Huang, A.; Tang, P.; Lin, H.; Liao, Y.; Liang, Y.; Ni, J.; Yan, P. Design, Synthesis, and Evaluation of a Series of Novel Super Long-Acting DPP-4 Inhibitors for the Treatment of Type 2 Diabetes. *J. Med. Chem.* **2020**, *63*, 7108–7126.

(8) a) Levitre, G.; Dagousset, G.; Anselmi, E.; Tuccio, B.; Magnier, E.; Masson, G. Four-Component Photoredox-Mediated Azidoalkoxy-Trifluoromethylation of Alkenes. *Org. Lett.* **2019**, *21*, 6005–6010. b) Zhang, L.; Zhang, G.; Wang, P.; Li, Y.; Lei, A. Electrochemical Oxidation with Lewis-Acid Catalysis Leads to Trifluoromethylative Difunctionalization of Alkenes Using CF₃SO₂Na. *Org. Lett.* **2018**, *20*, 7396–7399. c) Jud, W.; Kappe, C. O.; Cantillo, D. Catalyst-Free Oxytrifluoromethylation of Alkenes through Paired Electrolysis in Organic-Aqueous Media. *Chem. Eur. J.* **2018**, *24*, 17234–17238. d) Valverde, E.; Kawamura, S.; Sekine, D.; Sodeoka, M. Metal-Free Alkene Oxy- and Amino-Perfluoroalkylations via Carbocation Formation by Using Perfluoro Acid Anhydrides: Unique Reactivity between Styrenes and Perfluoro Diacyl Peroxides. *Chem. Sci.* **2018**, *9*, 7115–7121. e) Yang, Y.; Liu, Y.; Jiang, Y.; Zhang, Y.; Vicić, D. A. Manganese-Catalyzed Aerobic Oxytrifluoromethylation of Styrene Derivatives Using CF₃SO₂Na as the Trifluoromethyl Source. *J. Org. Chem.* **2015**, *80*, 6639–6648. f) Smirnov, V. O.; Maslov, A. S.; Kokorekin, V. A.; Korlyukov, A. A.; Dilman, A. D. Photoredox Generation of the Trifluoromethyl Radical from Borate Complexes via Single Electron Reduction. *Chem. Commun.* **2018**, *54*, 2236–2239. g) Li, Y.; Studer, A. Transition-Metal-Free Trifluoromethylaminooxylation of Alkenes. *Angew. Chem. Int. Ed.* **2012**, *51*, 8221–8224. h) Yasu, Y.; Koike, T.; Akita, M. Three-component Oxytrifluoromethylation of Alkenes: Highly Efficient and Regioselective Difunctionalization of C=C Bonds Mediated by Photoredox Catalysts. *Angew. Chem. Int. Ed.* **2012**, *51*, 9567–9571.

(9) a) Wang, P.; Zhu, S.; Lu, D.; Gong, Y. Intermolecular Trifluoromethyl-Hydrazination of Alkenes Enabled by Organic Photoredox Catalysis. *Org. Lett.* **2020**, *22*, 1924–1928. b) Zhu, C.-L.; Wang, C.; Qin, Q.-X.; Yruegas, S.; Martin, C. D.; Xu, H. Iron(II)-Catalyzed Azido-trifluoromethylation of Olefins and N-Heterocycles for Expedient Vicinal Trifluoromethyl Amine Synthesis. *ACS Catal.* **2018**, *8*, 5032–5037. c) Zhang, Y.; Han, X.; Zhao, J.; Qian, Z.; Li, T.; Tang, Y.; Zhang, H.-Y. Synthesis of β -Trifluoromethylated Alkyl Azides via a Manganese-Catalyzed Trifluoromethylazidation of Alkenes with CF₃SO₂Na and TMSN₃. *Adv. Synth. Catal.* **2018**, *360*, 2659–2667. d) Wang, F.; Qi, X.; Liang, Z.; Chen, P.; Liu, G. Copper-Catalyzed Intermolecular Trifluoromethylazidation of Alkenes: Convenient Access to CF₃-Containing Alkyl Azides. *Angew. Chem. Int. Ed.* **2014**, *53*,

- 1881–1886. e) Dagousset, G.; Carboni, A.; Magnier, E.; Masson, G. Photoredox-Induced Three-Component Azido- and Aminotrifluoromethylation of Alkenes. *Org. Lett.* **2014**, *16*, 4340–4343. f) Yasu, Y.; Koike, T.; Akita, M. Intermolecular Aminotrifluoromethylation of Alkenes by Visible-Light-Driven Photoredox Catalysis. *Org. Lett.* **2013**, *15*, 2136–2139.
- (10) Chen, Q.; Qing, F.-L. Stereoselective Construction of the 1,1,1-Trifluoroisopropyl Moiety by Asymmetric Hydrogenation of 2-(Trifluoromethyl)Allylic Alcohols and Its Application to the Synthesis of a Trifluoromethylated Amino Diol. *Tetrahedron* **2007**, *63*, 11965–11972.
- (11) Trost, B. M.; Wang, Y.; Hung, C.-I. J. Use of α -Trifluoromethyl Carbanions for Palladium-Catalysed Asymmetric Cycloadditions. *Nat. Chem.* **2020**, *12*, 294–301.
- (12) a) Franck, X.; Seon-Meniel, B.; Figadère, B. Highly Diastereoselective Aldol Reaction with α -CF₃-Substituted Enolates. *Angew. Chem. Int. Ed.* **2006**, *45*, 5174–5176. b) Shimada, T.; Yoshioka, M.; Konno, T.; Ishihara, T. Highly Stereoselective TiCl₄-Catalyzed Evans–Aldol and Et₃Al-Mediated Reformatsky Reactions. Efficient Accesses to Optically Active Syn- or Anti- α -Trifluoromethyl- β -Hydroxy Carboxylic Acid Derivatives. *Org. Lett.* **2006**, *8*, 1129–1131.
- (13) Selected recent reviews: a) Cotman, A. E. Escaping from Flatland: Stereoconvergent Synthesis of Three-Dimensional Scaffolds via Ruthenium(II)-Catalyzed Noyori–Ikariya Transfer Hydrogenation. *Chem. Eur. J.* **2021**, *27*, 39–53. b) Betancourt, R. M.; Echeverría, P.-G.; Ayad, T.; Phansavath, P.; Ratovelomanana-Vidal, V. Recent Progress and Applications of Transition-Metal-Catalyzed Asymmetric Hydrogenation and Transfer Hydrogenation of Ketones and Imines through Dynamic Kinetic Resolution. *Synthesis* **2021**, *53*, 30–50. c) Echeverría, P.-G.; Ayad, T.; Phansavath, P.; Ratovelomanana-Vidal, V. Recent Developments in Asymmetric Hydrogenation and Transfer Hydrogenation of Ketones and Imines through Dynamic Kinetic Resolution. *Synthesis* **2016**, *48*, 2523–2539. d) Matsunami, A.; Kayaki, Y. Upgrading and Expanding the Scope of Homogeneous Transfer Hydrogenation. *Tetrahedron Lett.* **2018**, *59*, 504–513. e) Echeverría, P.-G.; Ayad, T.; Phansavath, P.; Ratovelomanana-Vidal, V. Asymmetric (Transfer) Hydrogenation of Substituted Ketones Through Dynamic Kinetic Resolution. In *Asymmetric Hydrogenation and Transfer Hydrogenation*; John Wiley & Sons, Ltd, 2021; pp 129–174.
- (14) Selected recent articles: a) Vyas, V. K.; Clarkson, G. J.; Wills, M. Sulfone Group as a Versatile and Removable Directing Group for Asymmetric Transfer Hydrogenation of Ketones. *Angew. Chem. Int. Ed.* **2020**, *59*, 14265–14269. b) Wang, F.; Yang, T.; Wu, T.; Zheng, L.-S.; Yin, C.; Shi, Y.; Ye, X.-Y.; Chen, G.-Q.; Zhang, X. Asymmetric Transfer Hydrogenation of α -Substituted- β -Keto Carbonitriles via Dynamic Kinetic Resolution. *J. Am. Chem. Soc.* **2021**, *143*, 2477–2483. c) Touge, T.; Nara, H.; Kida, M.; Matsumura, K.; Kayaki, Y. Convincing Catalytic Performance of Oxo-Tethered Ruthenium Complexes for Asymmetric Transfer Hydrogenation of Cyclic α -Halogenated Ketones through Dynamic Kinetic Resolution. *Org. Lett.* **2021**, *23*, 3070–3075. d) Touge, T.; Sakaguchi, K.; Tamaki, N.; Nara, H.; Yokozawa, T.; Matsumura, K.; Kayaki, Y. Multiple Absolute Stereocontrol in Cascade Lactone Formation via Dynamic Kinetic Resolution Driven by the Asymmetric Transfer Hydrogenation of Keto Acids with Oxo-Tethered Ruthenium Catalysts. *J. Am. Chem. Soc.* **2019**, *141*, 16354–16361. e) Gediya, S. K.; Clarkson, G. J.; Wills, M. Asymmetric Transfer Hydrogenation: Dynamic Kinetic Resolution of α -Amino Ketones. *J. Org. Chem.* **2020**, *85*, 11309–11330. f) Carmona, J. A.; Rodríguez-Franco, C.; López-Serrano, J.; Ros, A.; Iglesias-Sigüenza, J.; Fernández, R.; Lassaletta, J. M.; Hornillos, V. Atroposelective Transfer Hydrogenation of Biaryl Aminals via Dynamic Kinetic Resolution. Synthesis of Axially Chiral Diamines. *ACS Catal.* **2021**, *11*, 4117–4124. g) Zhang, Y.-M.; Zhang, Q.-Y.; Wang, D.-C.; Xie, M.-S.; Qu, G.-R.; Guo, H.-M. Asymmetric Transfer Hydrogenation of Rac- α -(Purin-9-yl)Cyclopentones via Dynamic Kinetic Resolution for the Construction of Carbocyclic Nucleosides. *Org. Lett.* **2019**, *21*, 2998–3002. h) Luo, Z.; Sun, G.; Wu, S.; Chen, Y.; Lin, Y.; Zhang, L.; Wang, Z. η^6 -Arene CH–O Interaction Directed Dynamic Kinetic Resolution – Asymmetric Transfer Hydrogenation (DKR-ATH) of α -Keto/Enol-Lactams. *Adv. Synth. Catal.* **2021**, *363*, 3030–3034. i) More, G. V.; Malekar, P. V.; Kalshetti, R. G.; Shinde, M. H.; Ramana, C. V. Ru-Catalyzed Asymmetric Transfer Hydrogenation of α -Acyl Butyrolactone via Dynamic Kinetic Resolution: Asymmetric Synthesis of Bis-THF Alcohol Intermediate of Darunavir. *Tetrahedron Lett.* **2021**, *66*, 152831.
- (15) a) Šterk, D.; Stephan, M.; Mohar, B. Highly Enantioselective Transfer Hydrogenation of Fluoroalkyl Ketones. *Org. Lett.* **2006**, *8*, 5935–5938. b) Cotman, A. E.; Cahard, D.; Mohar, B. Stereoarrayed CF₃-Substituted 1,3-Diols by Dynamic Kinetic Resolution: Ruthenium(II)-Catalyzed Asymmetric Transfer Hydrogenation. *Angew. Chem. Int. Ed.* **2016**, *55*, 5294–5298. c) Ros, A.; Magriz, A.; Dietrich, H.; Fernández, R.; Alvarez, E.; Lassaletta, J. M. Enantioselective Synthesis of Vicinal Halohydrins via Dynamic Kinetic Resolution. *Org. Lett.* **2006**, *8*, 127–130. d) Betancourt, R. M.; Phansavath, P.; Ratovelomanana-Vidal, V. Ru(II)-Catalyzed Asymmetric Transfer Hydrogenation of 3-Fluorochromanone Derivatives to Access Enantioenriched *cis*-3-Fluorochroman-4-ols through Dynamic Kinetic Resolution. *J. Org. Chem.* **2021**, *86*, 12054–12063. e) Wang, T.; Phillips, E. M.; Dalby, S. M.; Sirota, E.; Axnanda, S.; Shultz, C. S.; Patel, P.; Waldman, J. H.; Alwedi, E.; Wang, X.; Zawatzky, K.; Chow, M.; Padivitage, N.; Weisel, M.; Whittington, M.; Duan, J.; Lu, T. Manufacturing Process Development for Belzutifan, Part 5: A Streamlined Fluorination–Dynamic Kinetic Resolution Process. *Org. Process Res. Dev.* **2021**. <https://doi.org/10.1021/acs.oprd.1c00242>. f) Wehn, P. M.; Rizzi, J. P.; Dixon, D. D.; Grina, J. A.; Schlachter, S. T.; Wang, B.; Xu, R.; Yang, H.; Du, X.; Han, G.; Wang, K.; Cao, Z.; Cheng, T.; Czerwinski, R. M.; Goggin, B. S.; Huang, H.; Halfmann, M. M.; Maddie, M. A.; Morton, E. L.; Olive, S. R.; Tan, H.; Xie, S.; Wong, T.; Josey, J. A.; Wallace, E. M. Design and Activity of Specific Hypoxia-Inducible Factor-2 α (HIF-2 α) Inhibitors for the Treatment of Clear Cell Renal Cell Carcinoma: Discovery of Clinical Candidate (S)-3-((2,2-Difluoro-1-hydroxy-7-(methylsulfonyl)-2,3-dihydro-1H-inden-4-yl)oxy)-5-fluorobenzonitrile (PT2385). *J. Med. Chem.* **2018**, *61*, 9691–9721. g) Mohar, B.; Stephan, M.; Urleb, U. Stereoselective Synthesis of Fluorine-Containing Analogues of Anti-Bacterial Sanfetrinem and LK-157. *Tetrahedron* **2010**, *66*, 4144–4149. h) Tan, X.; Zeng, W.; Wen, J.; Zhang, X. Iridium-Catalyzed Asymmetric Hydrogenation of α -Fluoro Ketones via a Dynamic Kinetic Resolution Strategy. *Org. Lett.* **2020**, *22*, 7230–7233.
- (16) Prakash, G. K. S.; Paknia, F.; Vaghoo, H.; Rasul, G.; Mathew, T.; Olah, G. A. Preparation of Trifluoromethylated Dihydrocoumarins, Indanones, and Arylpropanoic Acids by Tandem Superacidic Activation of 2-(Trifluoromethyl)Acrylic Acid with Arenes. *J. Org. Chem.* **2010**, *75*, 2219–2226.
- (17) a) Hashiguchi, S.; Fujii, A.; Takehara, J.; Ikariya, T.; Noyori, R. Asymmetric Transfer Hydrogenation of Aromatic Ketones Catalyzed by Chiral Ruthenium(II) Complexes. *J. Am. Chem. Soc.* **1995**, *117*, 7562–7563. b) Haack, K.-J.; Hashiguchi, S.; Fujii, A.; Ikariya, T.; Noyori, R. The Catalyst Precursor, Catalyst, and Intermediate in the Ru^{II}-Promoted Asymmetric Hydrogen Transfer between Alcohols and Ketones. *Angew. Chem. Int. Ed.* **1997**, *36*, 285–288.
- (18) G. Nedden, H.; Zanotti-Gerosa, A.; Wills, M. The Development of Phosphine-Free “Tethered” Ruthenium(II) Catalysts for the Asymmetric Reduction of Ketones and Imines. *Chem. Rec.* **2016**, *16*, 2623–2643.
- (19) Hayes, A. M.; Morris, D. J.; Clarkson, G. J.; Wills, M. A Class of Ruthenium(II) Catalyst for Asymmetric Transfer Hydrogenations of Ketones. *J. Am. Chem. Soc.* **2005**, *127*, 7318–7319.
- (20) Touge, T.; Hakamata, T.; Nara, H.; Kobayashi, T.; Sayo, N.; Saito, T.; Kayaki, Y.; Ikariya, T. Oxo-Tethered Ruthenium(II) Complex as a Bifunctional Catalyst for Asymmetric Transfer Hydrogenation and H₂ Hydrogenation. *J. Am. Chem. Soc.* **2011**, *133*, 14960–14963.
- (21) Kišić, A.; Stephan, M.; Mohar, B. *ansa*-Ruthenium(II) Complexes of R₂NSO₂DPEN-(CH₂)_n(η^6 -Aryl) Conjugate Ligands for Asymmetric Transfer Hydrogenation of Aryl Ketones. *Adv. Synth. Catal.* **2015**, *357*, 2540–2546.
- (22) a) Rast, S.; Modéc, B.; Stephan, M.; Mohar, B. γ -Sultam-Cored *N,N*-Ligands in the Ruthenium(II)-Catalyzed Asymmetric Transfer

Hydrogenation of Aryl Ketones. *Org. Biomol. Chem.* **2016**, *14*, 2112–2120. b) Jeran, M.; Cotman, A. E.; Stephan, M.; Mohar, B. Stereopure Functionalized Benzosultams via Ruthenium(II)-Catalyzed Dynamic Kinetic Resolution-Asymmetric Transfer Hydrogenation. *Org. Lett.* **2017**, *19*, 2042–2045. c) Cotman, A. E.; Lozinšek, M.; Wang, B.; Stephan, M.; Mohar, B. *trans*-Diastereoselective Ru(II)-Catalyzed Asymmetric Transfer Hydrogenation of α -Acetamido Benzocyclic Ketones via Dynamic Kinetic Resolution. *Org. Lett.* **2019**, *21*, 3644–3648.

(23) (*S,S*)-**2a** was obtained with (*S,S*)-DPEN based catalysts **C2**, **C3** and **C4**, and (*R,R*)-**2a** was obtained with (*R,R*)-**C1** and (*3R,1'S*)-**C5**.

(24) a) Dub, P. A.; Gordon, J. C. The Mechanism of Enantioselective Ketone Reduction with Noyori and Noyori-Ikariya Bifunctional Catalysts. *Dalton Trans.* **2016**, *45*, 6756–6781. b) Hall, A. M. R.; Berry, D. B. G.; Crossley, J. N.; Codina, A.; Clegg, I.; Lowe, J. P.; Buchard, A.; Hintermair, U. Does the Configuration at the Metal Matter in Noyori-Ikariya Type Asymmetric Transfer Hydrogenation Catalysts? *ACS Catal.* **2021**, *11*, 13649–13659.

(25) Using absolute rate theory, the ratio of the reaction rates on the two pathways is: $\ln(v_a/v_b) = \exp(-\Delta G_{298K}^\ddagger/RT)$, $RT = 0.59$ kcal·mol⁻¹

(26) $ee\ (\%) = 100 \times [\exp(-\Delta G_{298K}^\ddagger/RT) - 1] / [\exp(-\Delta G_{298K}^\ddagger/RT) + 1]$, where ΔG_{298K}^\ddagger is the free-energy difference in kcal·mol⁻¹ between the transition states leading to *S*- and *R*-products, $RT = 0.59$ kcal·mol⁻¹

(27) a) Dub, P. A.; Tkachenko, N. V.; Vyas, V. K.; Wills, M.; Smith, J. S.; Tretiak, S. Enantioselectivity in the Noyori-Ikariya Asymmetric Transfer Hydrogenation of Ketones. *Organometallics* **2021**, *40*, 1402–1410. b) Ref. 38b

(28) For molar ratios of triethylamine larger than 0.4, the mixture is biphasic, for this, see Narita, K.; Sekiya, M. Vapor-Liquid Equilibrium for Formic Acid-Triethylamine System Examined by the Use of a Modified Still. Formic Acid-Trialkylamine Azeotropes. *Chem. Pharm. Bull.* **1977**, *25*, 135–140.

(29) Selected recent examples: a) Dub, P. A.; Matsunami, A.; Kuwata, S.; Kayaki, Y. Cleavage of N–H Bond of Ammonia via Metal-Ligand Cooperation Enables Rational Design of a Conceptually New Noyori-Ikariya Catalyst. *J. Am. Chem. Soc.* **2019**, *141*, 2661–2677. b) Barrios-Rivera, J.; Xu, Y.; Wills, M. Asymmetric Transfer Hydrogenation of Unhindered and Non-Electron-Rich 1-Aryl Dihydroisoquinolines with High Enantioselectivity. *Org. Lett.* **2020**, *22*, 6283–6287. c) Zheng, Y.; Clarkson, G. J.; Wills, M. Asymmetric Transfer Hydrogenation of O-Hydroxyphenyl Ketones: Utilizing Directing Effects That Optimize the Asymmetric Synthesis of Challenging Alcohols. *Org. Lett.* **2020**, *22*, 3717–3721. d) Westermeyer, A.; Guilamot, G.; Phansavath, P.; Ratovelomanana-Vidal, V. Synthesis of Enantioenriched β -Hydroxy- γ -Acetal Enamides by Rhodium-Catalyzed Asymmetric Transfer Hydrogenation. *Org. Lett.* **2020**, *22*, 3911–3914.

(30) Epimerization is significantly faster using a higher molar ratio of triethylamine. For epimerization kinetics study of α -substituted ketone in HCO₂H/Et₃N 3:2 or 5:2, see Ref. 15b

(31) Su, X.; Huang, H.; Yuan, Y.; Li, Y. Radical Desulfur-Fragmentation and Reconstruction of Enol Triflates: Facile Access to α -Trifluoromethyl Ketones. *Angew. Chem. Int. Ed.* **2017**, *56*, 1338–1341.

(32) Deb, A.; Manna, S.; Modak, A.; Patra, T.; Maity, S.; Maity, D. Oxidative Trifluoromethylation of Unactivated Olefins: An Efficient and Practical Synthesis of α -Trifluoromethyl-Substituted Ketones. *Angew. Chem. Int. Ed.* **2013**, *52*, 9747–9750.

(33) Lu, Y.; Li, Y.; Zhang, R.; Jin, K.; Duan, C. Highly Efficient Cu(I)-Catalyzed Trifluoromethylation of Aryl(Heteroaryl) Enol Acetates with CF₃ Radicals Derived from CF₃SO₂Na and TBHP at Room Temperature. *J. Fluorine Chem.* **2014**, *161*, 128–133.

(34) »There was nothing to integrate« in ¹⁹F NMR spectra at signal/noise > 3000, and in chiral HPLC or GC spectra of the samples with concentration of 0.5 mg/mL.

(35) Alazet, S.; Ismalaj, E.; Glenadel, Q.; Le Bars, D.; Billard, T. Acid-Catalyzed Synthesis of α -Trifluoromethylthiolated Carbonyl Compounds. *Eur. J. Org. Chem.* **2015**, 4607–4610.

(36) Liu, J.-B.; Xu, X.-H.; Qing, F.-L. Silver-Mediated Oxidative Trifluoromethylation of Alcohols to Alkyl Trifluoromethyl Ethers. *Org. Lett.* **2015**, *17*, 5048–5051.

(37) a) Goldberg, F. W.; Kettle, J. G.; Kogej, T.; Perry, M. W. D.; Tomkinson, N. P. Designing Novel Building Blocks Is an Overlooked Strategy to Improve Compound Quality. *Drug Discovery Today* **2015**, *20*, 11–17. b) Grygorenko, O. O.; Volochnyuk, D. M.; Vashchenko, B. V. Emerging Building Blocks for Medicinal Chemistry: Recent Synthetic Advances. *Eur. J. Org. Chem.* **2021**, 6478–6510. c) Boström, J.; Brown, D. G.; Young, R. J.; Keserü, G. M. Expanding the Medicinal Chemistry Synthetic Toolbox. *Nat. Rev. Drug Discovery* **2018**, *17*, 709–727.

(38) a) Tsoung, J.; Krämer, K.; Zajdlík, A.; Liébert, C.; Lautens, M. Diastereoselective Friedel-Crafts Alkylation of Hydronaphthalenes. *J. Org. Chem.* **2011**, *76*, 9031–9045. b) Cotman, A. E.; Modec, B.; Mohar, B. Stereoarrayed 2,3-Disubstituted 1-Indanols via Ruthenium(II)-Catalyzed Dynamic Kinetic Resolution-Asymmetric Transfer Hydrogenation. *Org. Lett.* **2018**, *20*, 2921–2924.

(39) a) Keylor, M. H.; Matsuura, B. S.; Stephenson, C. R. J. Chemistry and Biology of Resveratrol-Derived Natural Products. *Chem. Rev.* **2015**, *115*, 8976–9027. b) Karageorgis, G.; Foley, D. J.; Laraia, L.; Waldmann, H. Principle and Design of Pseudo-Natural Products. *Nat. Chem.* **2020**, *12*, 227–235.

(40) a) Tomašič, T.; Durcik, M.; Keegan, B. M.; Skledar, D. G.; Zajec, Ž.; Blagg, B. S. J.; Bryant, S. D. Discovery of Novel Hsp90 C-Terminal Inhibitors Using 3D-Pharmacophores Derived from Molecular Dynamics Simulations. *Int. J. Mol. Sci.* **2020**, *21*, 6898. b) Dernovšek, J.; Zajec, Ž.; Durcik, M.; Mašič, L. P.; Gobec, M.; Zidar, N.; Tomašič, T. Structure-Activity Relationships of Benzothiazole-Based Hsp90 C-Terminal-Domain Inhibitors. *Pharmaceutics* **2021**, *13*, 1283.

(41) a) Thompson, A. J.; Orué, A. I. C.; Nair, A. J.; Price, J. R.; McMurtrie, J.; Clegg, J. K. Elastically Flexible Molecular Crystals. *Chem. Soc. Rev.* **2021**, *50*, 11725–11740. b) Naumov, P.; Karothu, D. P.; Ahmed, E.; Catalano, L.; Commins, P.; Halabi, J. M.; Al-Handawi, M. B.; Li, L. The Rise of the Dynamic Crystals. *J. Am. Chem. Soc.* **2020**, *142*, 13256–13272. c) Commins, P.; Karothu, D. P.; Naumov, P. Is a Bent Crystal Still a Single Crystal? *Angew. Chem. Int. Ed.* **2019**, *58*, 10052–10060. d) Saha, S.; Mishra, M. K.; Reddy, C. M.; Desiraju, G. R. From Molecules to Interactions to Crystal Engineering: Mechanical Properties of Organic Solids. *Acc. Chem. Res.* **2018**, *51*, 2957–2967. e) Reddy, C. M.; Krishna, G. R.; Ghosh, S. Mechanical properties of molecular crystals—applications to crystal engineering. *CrystEngComm* **2010**, *12*, 2296–2314.

(42) a) Pisičić, M.; Biljan, I.; Kodrin, I.; Popov, N.; Soldin, Ž.; Đaković, M. Elucidating the Origins of a Range of Diverse Flexible Responses in Crystalline Coordination Polymers. *Chem. Mater.* **2021**, *33*, 3660–3668. b) Worthy, A.; Grosjean, A.; Pfrunder, M. C.; Xu, Y.; Yan, C.; Edwards, G.; Clegg, J. K.; McMurtrie, J. C. Atomic Resolution of Structural Changes in Elastic Crystals of Copper(II) Acetylacetonate. *Nat. Chem.* **2018**, *10*, 65–69. c) Thompson, A. J.; Price, J. R.; McMurtrie, J. C.; Clegg, J. K. The Mechanism of Bending in Co-Crystals of Caffeine and 4-Chloro-3-Nitrobenzoic Acid. *Nat. Commun.* **2021**, *12*, 5983. d) Feiler, T.; Michalchuk, A. A. L.; Schröder, V.; List-Kratochvil, E.; Emmerling, F.; Bhattacharya, B. Elastic Flexibility in an Optically Active Naphthalidenimine-Based Single Crystal. *Crystals* **2021**, *11*, 1397.

(43) a) Reddy, C. M.; Gundakaram, R. C.; Basavoju, S.; Kirchner, M. T.; Padmanabhan, K. A.; Desiraju, G. R. Structural basis for bending of organic crystals. *Chem. Commun.* **2005**, 3945–3947. b) Reddy, C. M.; Padmanabhan, K. A.; Desiraju, G. R. Structure-Property Correlations in Bending and Brittle Organic Crystals. *Cryst. Growth Des.* **2006**, *6*, 2720–2731. c) Bhandary, S.; Thompson, A. J.; McMurtrie, J. C.; Clegg, J. K.; Ghosh, P.; Mangalampalli, S. R. N. K.; Takamizawa, S.; Chopra, D. The Mechanism of Bending in a Plastically Flexible Crystal. *Chem. Commun.* **2020**, 12841–12844.

(44) For a qualitative comparison of elastic flexibility of **2d** and **4d**, see attached “Movie 2d” and “Movie 4d”.

